ELSEVIER

Chemical Engineering Journal 116 (2006) 67–75

Chemical Engineering Journal

www.elsevier.com/locate/cej

Reactive NO absorption in aqueous Fe^{II}(EDTA) solutions in the presence of denitrifying micro-organisms

F. Gambardella, L.M. Galán Sánchez, K.J. Ganzeveld, J.G.M. Winkelman, H.J. Heeres *

Department of Chemical Engineering, Stratingh Institute, RijksUniversiteit Groningen, Nijenborgh 4, 9747 AG, Groningen, The Netherlands

Received 1 April 2005; received in revised form 7 October 2005; accepted 7 October 2005

Abstract

The effect of the presence of denitrifying biomass on the reactive absorption of NO in aqueous Fe^{II}(EDTA) solutions has been investigated (T = 303, 325 K, $C_{Fe^{II}(EDTA)}$ = 30–35 mol/m^3, $C_{\text{total solids}}$ = 0–7.5 kg/m^3, $C_{\text{suspended solids}}$ = 0–1.2 kg/m^3, $C_{\text{NO in}}$ = 250 vppm). The absorption rate of NO is affected by the presence of the biomass sludge and high sludge loadings resulted in reductions in the NO absorption rates. The decrease is likely due to partial blockage of the gas–liquid interface by inorganic and organic suspended solids and to a lesser extent to changes in the physical properties of the liquid. For one of the samples, an enhancement of the NO absorption rate was observed, presumably as a result of a shuttling effect due to the presence of small, adsorptive particles. A semi-empirical engineering model was developed based on the theory of mass transfer in combination with solid particles. The model includes both possible enhancement of mass transfer due to the presence of small adsorptive particles as well as reduction of the mass transfer rate due to the presence of particles adhering to the gas–liquid interface. The experimental profiles were modeled successfully using this approach.

Keywords: NO absorption; Solid particles; Shuttling effect; BiodeNOx

1. Introduction

Nitrogen monoxide plays an important role in the formation of ground-level ozone in highly populated areas and acid depositions. In the last decades, technologies have been developed to reduce NO emissions from various industrial activities. Combustion modification resulted in NO removal efficiencies of up to 70%. End of pipe technologies, like selective catalytic reduction (SCR) and selective non-catalytic reduction (SNCR), have been developed with high removal levels [1]. However, there is still a strong incentive for the development of low cost alternatives. Wet removal techniques, e.g. reactive NO absorption in Fe^{II}(EDTA) (EDTA = ethylenediaminetetraacetic acid) or Fe^{II}(NTA) (NTA = nitrilotriacetic acid) solutions offers promising possibilities [2,3]. Of particular interest is the so called BiodeNOx process, which combines reactive absorption of NO in an iron-chelate solution (Eq. (1)) followed by biological regeneration using denitrifying bacteria (Eq. (2))

$$Fe^{II}(EDTA)^{2-} + NO \rightleftarrows Fe^{II}(EDTA)(NO) \quad (1)$$

$$6Fe^{II}(EDTA)(NO) + C_2H_5OH \rightarrow 6Fe^{II}(EDTA) + 3N_2 + 2CO_2 + 3H_2O \quad (2)$$

The absorption and the regeneration may either be performed in two separate reactors, with the loaded Fe solutions flowing continuously from the absorber unit to the bioreactor, or in a combined operation [4].

Absorber performance is expected to be influenced by the presence of insoluble organic particles like the micro-organisms, inorganic particles and soluble organic and inorganic compounds (e.g. metabolic secretion products and salts). The reactor hydrodynamics and particularly the volumetric liquid side mass transfer coefficient k_La may be affected by these factors. Both positive and negative effects of biomass on mass transfer rates in gas–liquid systems have been reported [5–7].

Unfortunately, general expressions for k_La in bioreactors are lacking and the effects of biomass on the rate of gas absorption

* Corresponding author. Fax: +31 50 363 4479.
E-mail address: h.j.heeres@rug.nl (H.J. Heeres).

1385-8947/$ – see front matter © 2005 Elsevier B.V. All rights reserved.
doi:10.1016/j.cej.2005.10.012

Nomenclature

a	specific interfacial area ($m^2\,m^{-3}$)
A^0	area of the interface (m^2)
C	concentration ($mol\,m^{-3}$)
C_{NO}	concentration gas component (vppm)
C_{SS}	concentration of suspended solids (kg/m^3)
C_{TS}	concentration of total solid (kg/m^3)
C_{VS}	concentration of volatile solids (kg/m^3)
C_{VSS}	concentration of volatile suspended solid (kg/m^3)
d_S	diameter stirrer (m)
D	diffusion coefficient ($m^2\,s^{-1}$)
f_α, f_β	fraction of solids that participate in surface blocking and in grazing, respectively
J_{NO}	molflux of nitrogen monoxide ($mol\,m^{-2}\,s^{-1}$)
$J_{NO}A$	absorption rate of nitrogen monoxide ($mol\,s^{-1}$)
k_L	mass transfer coefficient for the liquid phase ($m\,s^{-1}$)
K_α, K_β	surface adsorption equilibrium constants
N_S	stirrer speed (s^{-1})
Re	Reynolds number ($\rho N_S d_S \mu^{-1}$)
Sc	Schmidt number ($\mu \rho^{-1} D^{-1}$)
Sh	Sherwood number ($d_S k_L D^{-1}$)
t	time (s)
T	temperature (K)
V	volume (m^3)

Greek letters

$\alpha_{max}, \beta_{max}$	maximum fractional surface coverage with blocking and grazing, respectively
Φ	volumetric flow rate ($m^3\,s^{-1}$)
μ	dynamic viscosity (Pa s)
ν	kinematic viscosity ($m^2\,s^{-1}$)
ρ	density (kg/m^3)

Subscripts

exp	experimental value
G	gas phase
in	inlet
L	liquid phase
NO	nitrogen monoxide
out	outlet
w	water

Superscript

b	bulk
0	value without solid present

appeared to be case specific. Expressions from literature that model the influence of solids on mass transfer in gas–liquid reactors always contain one or more parameters that have to be found via fitting of experimental results. This is the case in the presence of only a single type of solid particles of a uniform size and with a well defined regular shape, let alone in the presence of a complex biologically active sludge with various types of solids present.

In the present work, the effect of the presence of biological sludge on the absorption of NO in aqueous Fe^{II}(EDTA) solution was investigated. Three representative sludge solutions were tested: a denitrifying sludge from a waste water treatment plant and two BiodeNOx sludge solution from different origins. The NO absorption rates were investigated as a function of the concentration of biological sludge using typical BiodeNOx reaction conditions (T = 325 K, $C_{Fe^{II}(EDTA)}$ = 0–50 mol/m^3, pH 7, $C_{NO\,in}$ = 250 vppm, C_{VSS} = 0.2–2 kg/m^3). This research was not aimed at the microbiological properties of the sludge. The main goal, on the other hand, was to gain insight into the possible qualitative influences of the sludges on the engineering aspects of NO absorbers, and to demonstrate the ability of quantitative descriptions of the observed phenomena via semi-empirical models.

2. Experimental

2.1. Chemicals

Na_4-EDTA solution (39% in water) was obtained from Caldic Nederland, $FeSO_4{\cdot}7H_2O$ and $CeSO_4{\cdot}4H_2O$ (>99%) from Acros, Na_2CO_3 and H_2SO_4 (99%) from Merck, NaOH (33% in water) from Boom. NO (1008 vppm in N_2), and N_2 (>99.99%) were purchased from Hoekloos. Reverse osmosis water was applied to prepare the iron chelate solutions.

2.2. Experimental set-up

The kinetic experiments were carried out in a stirred cell reactor consisting of glass and equipped with four glass baffles. A stainless steel turbine impeller was used to stir the gas phase, while a magnetic stirrer bar in combination with an external magnetic drive was used to mix the liquid phase. The double wall of the reactors allowed the use of water to regulate the temperature in the reactor (Julabo, MV basis). Typical reactor dimensions are given in Table 1.

A temperature (PT-100) and pressure transducer (Trafag, ECO 2.5 A) were used to monitor the temperature and pressure during an experiment. The NO concentration in the outlet gas flow was measured using an NO analyzer (Thermo Electron-Model 10). The analyzer was calibrated before and after every experiment using the NO gas mixture at known concentration. The NO analyzer, the temperature and pressure transducer were connected to a computer equipped with a NI-4351 PCI (National instrument) data acquisition card. The reactor set-up is schematically represented in Fig. 1.

Table 1
Dimensions and characteristics of the stirred cell contactor

Reactor volume (m^3)	1.245×10^{-3}
A^0 (m^2)	7.79×10^{-3}
Φ_G (m^3/s)	8.33×10^{-6}
Liquid impeller	Magnetic stirrer d_S = 0.02 m
Gas impeller	Six bladed turbine d_S = 0.06 m
N_S liquid stirrer (min^{-1})	100
N_S gas impeller (min^{-1})	2000

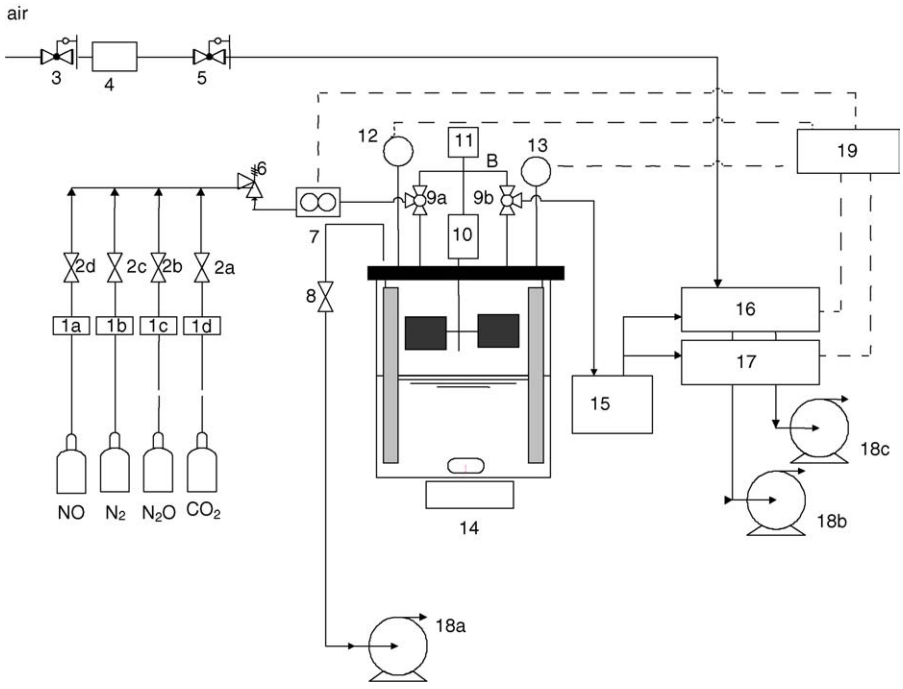

Fig. 1. Schematic representation of the experimental set-up. 1a, 1b, 1c, 1d: mass-flow controllers; 2a, 2b, 2c, 2d, 6, 8: open/close valves; 3, 4, 5: air valves and filter; 7: digital flowmeter; 9a, 9b: three way valves; B: bypass; 10, 11: magnetic coupling; 12: PT-100; 13: pressure transducer; 14: magnetic plate; 15: cold trap; 16: NO analyzer; 17: O_2 analyzer; 18a, 18b, 18c: vacuum pump; 19: pc.

2.3. Preparation of the aqueous sludge/Fe^{II}(EDTA) suspensions

Aqueous solutions of Fe^{II}(EDTA) are extremely air-sensitive and for this reason, the preparation was carried out under nitrogen. The Fe^{II}(EDTA) solution was prepared by diluting a predetermined amount of EDTA solution in approximately 10^{-4} m^3 of reverse osmosis water. The pH was brought from an initial value of 10–11 to 9 by the addition of a few drops of a 2 M H_2SO_4 solution. The appropriate amount of $FeSO_4{\cdot}7H_2O$ (Fe:EDTA ratio = 1:1.1 mol/mol) was added to the EDTA solution and the volume was brought to 9×10^{-4} m^3. Solutions of H_2SO_4 or NaOH were used to bring the pH to neutrality. Subsequently, water was added to adjust the total volume to 10^{-3} m^3. This amount of solution, maintained under nitrogen, was sufficient to perform several experiments. The biological sludge was activated by the addition of a drop of ethanol, homogenized and then diluted with reverse osmosis water to the pre-set biomass loading. The appropriate amount of the iron chelate solution was added to the biomass suspension to obtain the desired solid and iron chelate concentration for a particular experiment. The pH of the Fe^{II}(EDTA)/sludge suspensions was adjusted to 7 when necessary.

2.4. Biomass characteristics and handling

The first sample of denitrifying biomass was obtained from a waste water treatment plant (Veendam, The Netherlands). The dark brown sample contained solids in the form of small agglomerates and traces of sand. The other two samples consisted of BiodeNOx cultures form two different reactor set-ups. The first sample (Wageningen University, The Netherlands) was taken from a continuous reactor operated at typical BiodeNOx process conditions. This solution was used as such. The second BiodeNOx sample (University of Delft, The Netherlands) was cultivated and grown under BiodeNOx conditions in a batch reactor. This sample was concentrated by centrifugation and treated with a buffer solution (a mixture of Na_4-EDTA and *tris*(hydroxymethyl-aminomethane), pH 8) to preserve its biological activity. The biological sludge was stored at 4 °C. A sample of 10^{-5} m^3 was used to measure the biological activity [8].

The total solid concentration of the biomass solution (C_{TS}) was determined by measuring the dry weight of a biomass sample (10^{-5} m^3) after it had been stored in an (electric) oven (Binder 9010-0078 2.0) at 103 °C for 24 h.

The volatile solid concentration (C_{VS}) was determined by placing a sample in an (electric) oven (Heraeus D-6450 Hanau) at 600 °C for 3 h The C_{VS} may be calculated from the C_{TS} value and the residual mass after the high temperature treatment.

The concentration of suspended solids (C_{SS}) was obtained by filtration of the sludge sample under vacuum (Pall-Supor 200-0.2 μm) followed by drying of the residue in an (electric) oven at 103 °C for 24 h.

The determination of the volatile suspended solid concentration (C_{VSS}) was performed by placing the residue of a filtered sample in an oven at 600 °C for 3 h. The C_{VSS} of the sample may be calculated from the C_{SS} and the weight of the residue [9].

The measurements were performed on sludge samples before addition to the Fe^{II}(EDTA) solutions.

2.5. Description of a typical reactive absorption experiment

Reactive absorption experiments were carried in the stirred cell contactor in a batch mode with respect to the liquid phase and in a continuous mode with respect to the gas phase. The reactor was filled with the appropriate solution (iron chelate solution, biomass and water, pH 7). Before closing it, a sample (1×10^{-5} m^3) was taken from the reactor to determine the concentration of Fe^{II}(EDTA). The reactor content was degassed under vacuum for about 15 min. After degassing, the reactor was filled with nitrogen gas until atmospheric pressure was reached. The reactor content was heated to the desired temperature. A mixture gas of NO in N_2 was prepared and bypassed around the reactor to the NO analyzer. The NO concentration in the gas phase was regulated using the mass flow controllers and the composition of the mixture gas was determined using the NO analyzer. Subsequently, the reaction was initiated by closing the bypass valves and admitting the gas mixture to the reactor. The NO concentration of the outlet flow was monitored as a function of the time.

2.6. Determination of the Fe^{II} content in the solution

The concentration of Fe^{II} in the solution was determined by a titration with a 0.1 M $Ce(SO_4)_2$ solution. A 0.025 M ferroine solution was used as indicator [10]. In order to obtain reproducible results, the iron-chelate sample was diluted with an approximate 10-fold volume of sulfuric acid (2–4 kmol/m^3), and degassed by the addition of approximately 1 g of $NaHCO_3$.

2.7. Analytical measurements

The kinematic viscosity, ν, of the iron chelate solution in presence and in absence of biomass, was measured with a glass Ubbelohde viscometer (PSL-SSLC-2-1505). The densities of the solutions were determined using an electronic balance (Mettler PM 2000). These measurements allowed the calculation of the relative dynamic viscosity of the iron chelate solution in the presence and absence of biomass using

$$\frac{\mu}{\mu_w} = \frac{\rho\nu}{\rho_w\nu_w} \tag{3}$$

Electron microscopy was performed using a Philips CM120 operated at 120 kV, a magnitude of 3000/3800 and using a Gatan 794 Slow-Scan CCD Camera.

3. Theory; determination of the NO absorption rate

For our set-up, a mass balance for NO for the gas phase leads to

$$V_G \frac{dC^b_{NO,G}}{dt} = \Phi_G(C_{NO\,in} - C^b_{NO,G}) - (J_{NO}A)_{exp} \tag{4}$$

When the absorption process reaches a pseudo steady state (see Fig. 4, the outgoing NO concentration is almost constant after 300–400 s), the NO concentration in the bulk of the gas phase, $C^b_{NO,G}$ is constant and equal to $C_{NO\,out}$ and Eq. (4) simplifies to

$$(J_{NO}A)_{exp} = \Phi_G(C_{NO\,in} - C_{NO\,out}) \tag{5}$$

$C_{NO\,in}$, $C_{NO\,out}$ and and Φ_G are measured continuously, allowing determination of the absorption rate of NO, $(J_{NO}A)_{exp}$.

4. Results and discussion

4.1. Biomass characteristics

In this study, the effects of the presence of three different types of biomass sludges on the NO absorption rate in aqueous Fe^{II}(EDTA) solutions were tested. An overview of the characteristics of the different biomass solutions is given in Table 2. The first sample was obtained from a waste water treatment plant and contains denitrifying bacteria. The other two samples consisted of typical BiodeNOx cultures, arising from different reactor set-ups. The micro-organisms present in the BiodeNOx process consist of a.o. iron reducing bacteria to perform the reduction of the ferric chelate complex and denitrifying micro-organisms for the regeneration of the Fe^{II}(EDTA)-NO complex. The biomass was tested on activity before preparation of the reactive absorption solutions and all showed considerable activity.

The major difference between sample 2 and sample 3 is the amount of suspended solids and particularly the C_{VSS}. This indicates that the amount of insoluble organic matter (e.g. in the form of metabolites and dead or alive micro-organisms) in sample 3 is a factor 7 higher than in sample 2. This is confirmed by electron microscopy images (Figs. 2 and 3). Qualitatively, the number of small solid particles (<1 μm) and micro-organisms in sample 3 is significantly higher than in sample 2. In addition, the imagines also allow determination of typical cell sizes, which is in the order of 1 μm.

Table 2
Characteristics of the biomass sludges

#	C_{TS} (kg/m^3)	C_{VS} (kg/m^3)	C_{SS} (kg/m^3)	C_{VSS} (kg/m^3)	$C_{Fe^{III}(EDTA)}$[a] (mol/m^3)	pH
1	5.5	3.6	n.d.	n.d.	0	7
2	22.5	6.8	0.9	0.5	25	7
3	22.6	10.1	3.8	3.4	150	8

n.d.: not determined.
[a] Based on the intakes in the original reactor-set-ups.

Table 3
Experimental overview

T (K)	Biomass #	Biomass status	C_{TS} (kg/m^3)	C_{SS} (kg/m^3)	$C_{Fe^{II}(EDTA)}$ (mol/m^3)	$C_{NO\,in}$ (vppm)	$C_{NO\,out}$ [a] (vppm)
303	1	Pure	0	n.d.	35	264	74
			0.39	n.d.	35	260	112
			0.45	n.d.	35	261	98
			0.47	n.d.	35	262	95
			0.60	n.d.	35	263	103
			1.04	n.d.	35	266	123
		Filtered	0.57[b]	0	35	264	76
			1.57[b]	0	35	258	74
			1.57[b]	0	35	262	76
			1.87[b]	0	35	263	79
325	2	Pure	0	0	30	262	112
			0.75	0.03	30	264	112
			1.50	0.06	30	262	124
			1.50	0.06	30	263	126
			3	0.12	30	262	127
			4.5	0.19	30	263	129
			6	0.25	30	265	131
325	3	In buffer	0	0	30	260	107
			0.76	0.13	30	250	103
			1.5	0.25	30	262	105
			1.5	0.25	30	259	104
			3.01	0.50	30	260	110
			3.75	0.63	30	261	110
			6.02	1.01	30	265	125
			7.52	1.26	30	259	134

[a] Values measured after 500 s absorption time.
[b] Values before filtration.

4.2. Absorption experiments

NO absorption experiments in aqueous Fe^{II}(EDTA) solutions in the presence of biological sludge were performed in a stirred cell contactor. Typical profiles obtained for absorption experiments are shown in Fig. 4. Rapid concentration changes takes place in the first stage of the experiment due to reactor dynamics. Subsequently, reactive absorption takes place and a slow increase of the NO concentration in the outlet is observed. In this stage, $C_{Fe^{II}(EDTA)}$ slowly decreases due to the reaction with NO, leading to a slow decrease in the absorption rates. However, the total Fe^{II} conversion in a typical experiment is less

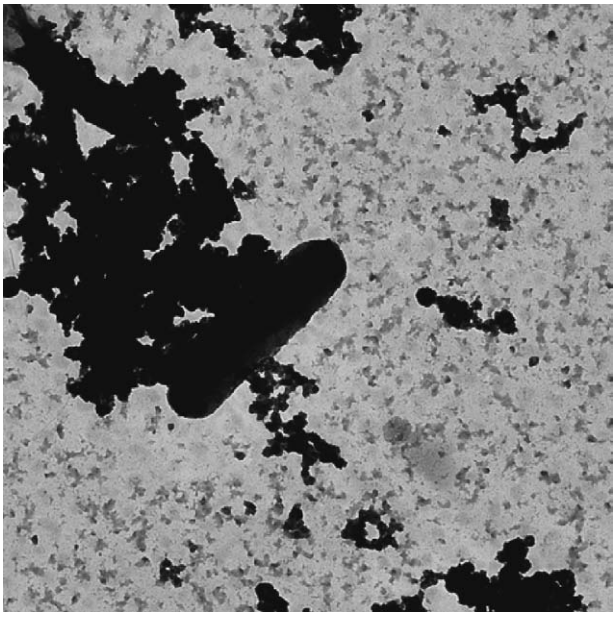

Fig. 2. Electron microscopy image of the BiodeNOx sample 2.

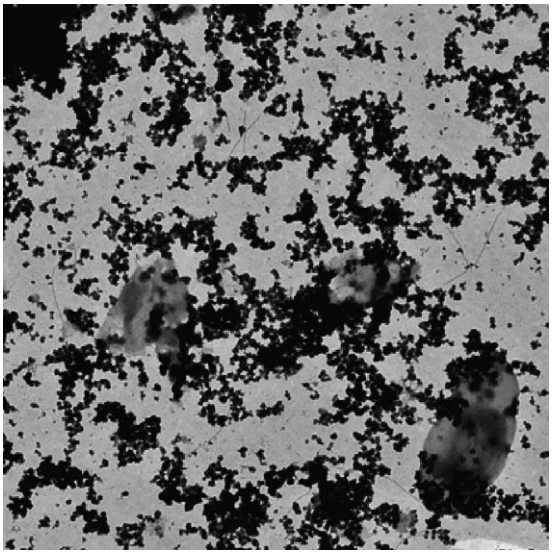

Fig. 3. Electron microscopy image of BiodeNOx sample 3.

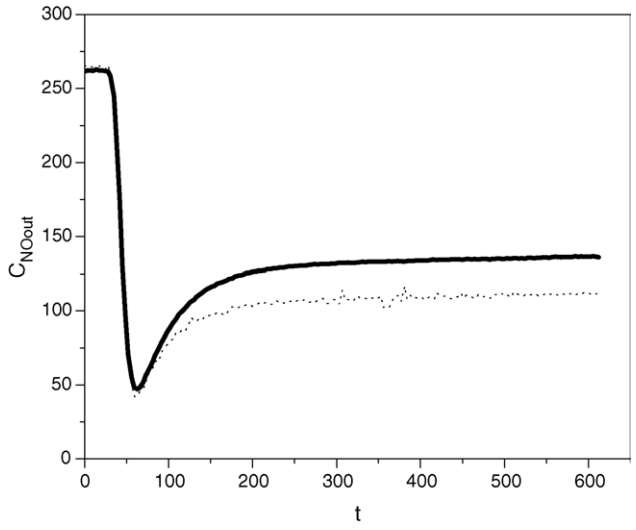

Fig. 4. Typical NO concentration profiles with and without biomass. $T = 323$ K, $C_{NO\,in} = 260$ ppmv, pH 7, $C_{Fe^{II}(EDTA)} = 30$ mol/m^3. Dotted line: no biomass. Solid line: with biomass, $C_{TS} = 7.52$ kg/m^3 (sample 3).

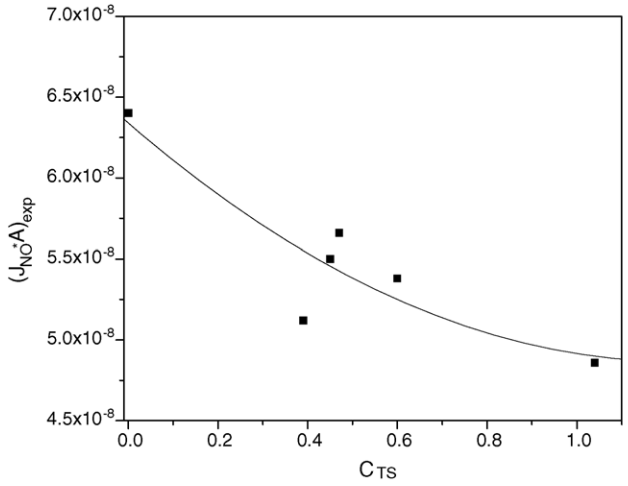

Fig. 5. Absorption rate of NO in Fe^{II}(EDTA) solutions as a function of the C_{TS} (sample 1). $C_{Fe^{II}(EDTA)} = 35$ mol/m^3, $T = 303$ K, $C_{NO\,in} \approx 260$ vppm. Line: for illustrative purposes only.

than 5% and it is safe to assume a pseudo steady state situation with a nearly constant $C_{Fe^{II}(EDTA)}$ and J_{NO}. The absorption process is affected by the addition of various amounts of sludge, see Fig. 4 for details. An overview of all experiments is given in Table 3.

4.3. Experiments with sample 1

Initial experiments were carried out with a sludge sample form a waste water plant (sample 1). It contains various denitrifying micro-organisms. In contrast to BiodeNOx sludge, it was abundantly available for testing and was therefore studied in more detail. The reactive NO absorption experiments with this biomass solution were carried out at 303 K. Higher temperatures were not possible due to excessive foam formation. The absorption rate of NO as a function of the total solid loading is given in Fig. 5. The absorption rate decreases considerably with increasing C_{TS}.

The observed trend may be a consequence of the presence of insoluble suspended solids like micro-organisms or small particles in the biomass solution. These are known to affect gas absorption rates. It is also possible that the mass transfer rate is reduced by the presence of soluble compounds in solution. These are expected to have an effect on the physical properties of the reaction medium (e.g. surface tension and viscosity) and as such may affect the mass transfer coefficients.

In order to test whether the NO absorption rates are affected by the presence of insoluble material a group of experiments was performed using filtered biomass sample 1. The results are given in Fig. 6.

The absorption rate of NO decreases slightly when increasing the amount of filtered biomass medium. However, the decrease is much lower than observed when using the original, unfiltered solution. This suggests that the insoluble particles and microorganisms are primary responsible for the decrease in the NO absorption rates and that the composition/properties of the liquid phase is of less importance. Negative effects on mass transfer rates by inert particles have been reported in the literature [11–14]. A possible explanation is the adherence of the particles to the gas–liquid interface, which lowers the effective gas–liquid interfacial area available for gas absorption (vide infra).

Excessive Fe^{II}(EDTA) oxidation due to the presence of the biomass and the formation of Fe^{III}(EDTA), which is not capable of binding NO and thus will also lead to reduced absorption rates, can be excluded. In a separate experiment, the Fe^{II}(EDTA) concentration in the presence of biological sludge in the absence of NO and oxygen was followed as a function of the time. The concentration of Fe^{II}(EDTA) did not vary considerably, indicating that Fe^{II}(EDTA) is not oxidized rapidly by the biological sludge.

4.4. Experiments with BiodeNOx samples 2 and 3

A number of NO absorption experiments was carried out in the presence of variable amounts of the BiodeNOx samples 2 and

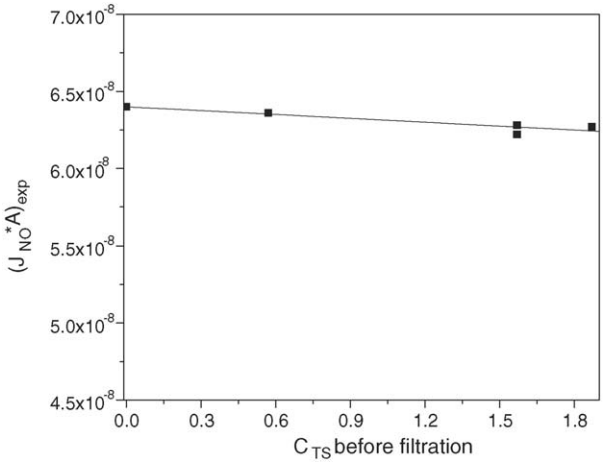

Fig. 6. Absorption rate of NO in Fe^{II}(EDTA) solutions using filtered biomass of sample 1. $T = 303$ K, $C_{Fe^{II}(EDTA)} = 35$ mol/m^3, $C_{NO\,in} \approx 260$ vppm, pH 7.

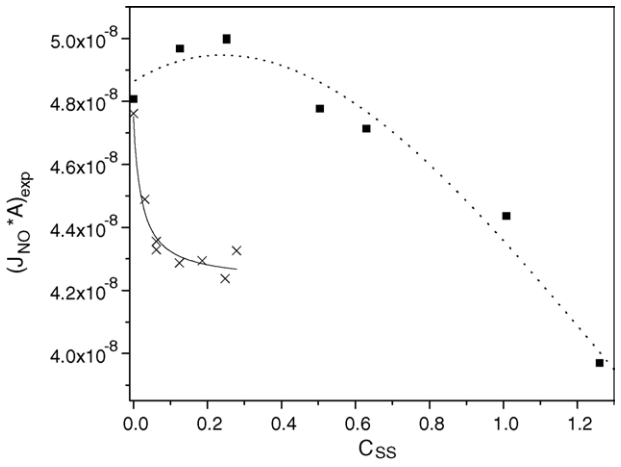

Fig. 7. Absorption rates of NO in Fe^{II}(EDTA) solutions in presence of biomass sample 2 (×) and sample 3 (■). $T = 325$ K, $C_{Fe^{II}(EDTA)} = 30$ mol/m^3, $C_{NO\,in} \approx 260$ vppm, pH 7. Solid line: based on Eq. (11). Dotted line: based on Eq. (10).

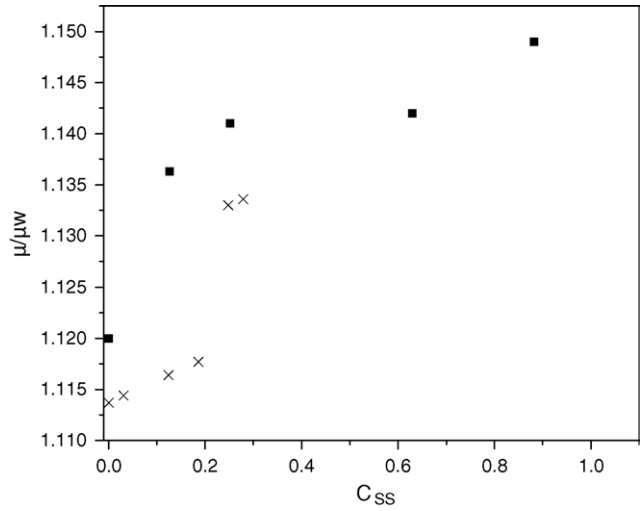

Fig. 8. Relative viscosity of aqueous Fe^{II}(EDTA) solutions in the presence of different concentrations of biological sludge; sample 2 (×), sample 3 (■). $T = 325$ K, $C_{Fe^{II}(EDTA)} = 30$ mol/m^3, pH 7.

3 ($T = 325$ K, $C_{Fe^{II}(EDTA)} = 30$ mol/m^3, $C_{NO\,in} \approx 260$ vppm, pH 7). The absorption rate of NO through the gas–liquid interface was determined as a function of the C_{SS}. The results are given in Fig. 7.

It is clear that the absorption rate of NO through the gas–liquid interface is reduced considerably in the presence of high concentrations of BiodeNOx sludge. For instance, for sample 3, the absorption rate of NO is reduced with about 20%, i.e. from 4.8×10^{-8} mol/s to 4.0×10^{-8} mol/s at a C_{SS} of 1.25 kg/m^3. The experimental profiles for both samples show distinct differences. In case of sample 2, a small C_{SS} (<0.2 kg/m^3) already results in a large decrease in the NO absorption rate. The effect levels off at higher C_{SS} values. In case of sample 3, a small increase in the absorption rate of NO is observed at low C_{SS} (0–0.3 kg/m^3). This effects levels off at a C_{SS} of about 0.3 kg/m^3. A subsequent increase in the solid loadings result in a considerable decrease in the NO absorption rate. As observed with sample 1, it is likely that the observed effects are due to the presence of suspended solids like micro-organisms and solid particles in the liquid phase. These may influence the gas absorption rates in different ways, i.e. by affecting the overall viscosity of the liquid and thus the k_L [14,15], by blocking the interface and effectively reducing the interfacial area available for mass transfer [13], and/or by enhancing the rate of NO absorption due to the presence of small absorptive particles [11,17].

To study the possible effects of the viscosity, the relative viscosity of (diluted) sludge samples 2 and 3 were measured and the results are given in Fig. 8. For both samples, the viscosity increases with increasing C_{SS}. For sample 3, the relative viscosity increases with about 2.7% when increasing the C_{SS} from 0 to 1 kg/m^3. These viscosity effects may have an impact on k_L and as such on the mass transfer rates. The magnitude of these effects may be evaluated by considering a typical dimensionless equation that correlates the k_L with a.o. the liquid viscosity [16]

$$Sh = c\,Re^{n}\,Sc^{0.33} \quad (6)$$

For a stirred vessel, typical values for n are between 0.8 and 1. According to Eq. (6), an increase in the viscosity of 2.7% will lead to a marginal decrease in the k_L (<2%). This is far too low to explain the experimentally observed reductions in the absorption rate of NO in the presence of biomass sludge. Thus, reduction of the NO absorption rates due to viscosity effects are highly unlikely. These results are also in line with those obtained for sample 1 (vide supra).

The observed reductions of J_{NO} in the presence of sludge is more likely due to the presence of suspended solids. These may affect the mass transfer of gasphase component to the liquid phase in various ways. Reductions in mass transfer rates have been reported due to a reduction of the gas–liquid interfacial area, a result of the presence of the suspended solids which (partially) adhere to the gas–liquid interface [12,13]. However, enhancement of mass transfer rates is also possible. It has been reported in the literature that low concentrations of small solids in solution may enhance the gas absorption rate (grazing or shuttling effect) [11,13,17]. Enhancement factor values up to 8 have been observed. To be effective, the particles have to be considerably smaller than the liquid side mass transfer layer and need to have a high affinity for the component to be transferred [11]. Typically, a sharp increase in the mass transfer rate versus the solids loading is observed followed by a leveling of to a constant value. The minimum solids loading for maximum enhancement is system dependent and varies between 0.2 and 10 kg/m^3 [16]. A shuttling type of mechanism has been proposed to explain these phenomena.

For sample 2, mass transfer enhancement due to the presence of sludge is not observed (Fig. 7). It suggests that small adsorptive particles are absent. The observed trend is indicative for the presence of solids (organic, inorganic, micro-organisms) which adhere to the gas–liquid interface and effectively reduce the interfacial area.

The experimental results for BiodeNOx sample 3 (Fig. 7) suggest that both mechanisms (shuttling and particle block-

ing) are operative, leading to mass transfer enhancement at low solids concentrations and reductions at high solids loading. The sample contains a variety of solids with different sizes and properties (Fig. 3). It is well possible that the larger solid particles (inorganics or even micro-organisms) are involved in surface blocking and that the smaller solids of either organic or inorganic origin (iron or iron oxides) play a role in the shuttling process. The range of C_{SS} for which mass transfer enhancement is observed (0–0.3 kg/m^3) is within the range reported in the literature (0–10 kg/m^3).

4.5. Development of a semi-empirical model for mass transfer in the presence of suspended solids

A general expression for the molflow of NO in the presence of particles may be given by

$$(J_{NO}A)_{exp} = \left(1 - \frac{\alpha_{max} K_\alpha f_\alpha C_{SS}}{1 + K_\alpha f_\alpha C_{SS}}\right) E_{NO,g} (J_{NO}A^0)_{C_{SS}=0} \quad (7)$$

The term containing α_{max} accounts for surface blocking and is represented by a Langmuir–Hinshelwood type of adsorption isotherm. The factor f_α is introduced to represent the fraction of solids that participate in surface blocking. The grazing effect is accounted for with an enhancement factor $E_{NO,g}$. Vinke [18] developed an analytical expression for $E_{NO,g}$ based on the film theory. With the assumption that the grazing particles remain far from saturated, this expression reduces to

$$E_{NO,g} = 1 + \beta \left(\frac{4D_{NO}}{d_p k_l} - 1\right) \quad (8)$$

where β denotes the surface fraction covered by grazing particles. Following Vinke [18], β can also be described using a Langmuir–Hinshelwood isotherm

$$\beta = \beta_{max} \frac{K_\beta f_\beta C_{SS}}{1 + K_\beta f_\beta C_{SS}} \quad (9)$$

We have introduced a factor f_β as the fraction of the solids that participate in the grazing effect. Combining the above equations gives

$$(J_{NO}A)_{exp} = \left(1 - \frac{aC_{SS}}{1 + K_a C_{SS}}\right)\left(1 + \frac{bC_{SS}}{1 + K_b C_{SS}}\right) \times (J_{NO}A^0)_{C_{SS}=0} \quad (10)$$

where the number of parameters is reduced to four, according to $a = \alpha_{max} K_\alpha f_\alpha$, $K_a = K_\alpha f_\alpha$, $b = \beta_{max} K_\beta f_\beta \left(\frac{4D_{NO}}{d_p k_l} - 1\right)$, and $K_b = K_\beta f_\beta$.

The observed molar flows of NO (Fig. 7) versus the particle concentrations for BiodeNOx samples 2 and 3 were modeled using Eq. (10).

In the case of sample 2, mass transfer enhancement due to grazing was not observed, indicating that f_β equals zero. In this case, Eq. (10) reduces to:

$$(J_{NO}A)_{exp} = \left(1 - \frac{aC_{SS}}{1 + K_a C_{SS}}\right)(J_{NO}A^0)_{C_{SS}=0} \quad (11)$$

The experimental data were modeled using this expression, leading to $a = 4.9$ and $K_a = 44.7$. The modeled data are in good agreement with the experimental data (Fig. 7). Hence, the experimental absorption rate of NO for sample 2 may be modeled satisfactorily when assuming that the NO absorption rate is reduced by suspended solids adhering to the gas–liquid interface.

In the case of sample 3, both grazing and particle adherance to the surface is observed and Eq. (10) was used to model the data. A least-squares fit of the experimental data yielded the following values: $a = 0.98$; $K_a = 0.80$; $b = 1.33$; $K_b = 0.33$. The experimental data and the modeled profile according to Eq. (10) is given in Fig. 7. Agreement between model and experimental data is very satisfactorily.

5. Conclusions

The absorption of NO in Fe^{II}(EDTA) solution in the presence of biological sludge was investigated. The molar flow of NO through the gas–liquid interface is a function of the type of biomass sludge and the sludge loading. In general, the molar flow of NO is reduced upon the addition of biomass sludge (max 30%). This effect is likely due to adherence of the suspended solids in the biomass sludge to the gas–liquid interface, effectively reducing the gas–liquid area available for mass transfer. For one of the BiodeNOx sludge samples, an increase of the NO molar flow was observed at a low C_{SS}. This could be due to the presence of small adsorptive particles in the biomass which are known to be able to enhance mass transfer.

At the same time, we can conclude that the magnitude, and even the direction (enhancing or decreasing), of the influence of biological sludge on the absorber performance depends on the amount of sludge present, but decisive as well are the type and origin of the sludge. Our results have clear implications for the design and operation of BiodeNOx (pilot)-units. It can be expected that at typical BiodeNOx solids loadings (C_{VSS} = 0.2–2 kg/m^3), the NO molar flow will be affected and most likely lowered compared to biomass free Fe^{II}(EDTA) solutions. Maintaining a low concentration of suspended solids in the absorber may limit these negative effects.

Acknowledgments

The research was financially supported by the Netherlands Technology Foundation (STW). Electron microscopy images were realized by W. Bergsma and G. Oostergetel of the Biophysics department, RijksUniversiteit Groningen, The Netherlands.

References

[1] T.F. Mc Gowan, Charting a path for cost-effective NO_x control. Chem. Eng., October 2004. http://www.che.com, New York.

[2] S.G. Chang, D. Littlejohn, The potential of a wet process for simultaneous control of SO_2 and NO_x in flue gas. Preprints of Paper Division of Fuel Chemistry, Am. C. 30 (1985) 119–124.
[3] K.J. Smith, S. Tseng, M. Babu, Enhanced NO_x removal in wet scrubbers using metal chleates, in: Proceedings of the 86th Air and Waste Management, Denver, USA, 1993.
[4] C.J. Buisman, H. Dijkman, P.L. Verbaak, A.J. Den Hartog, Process for purifying flue gas containing nitrogen oxides, WO 96/24434, 1996.
[5] K. Schugerl, Bioreaction Engineering, Characteristic Features of Bioreactors, vol. 2, Wiley, New York, 1991.
[6] J. Zahradnik, New Methodologies for multiphase bioreactors: hydrodynamic and mass transfer characteristics of multistage slurry reactors, in: Multiphase Bioreactor Design, Taylor and Francis, New York, 2001.
[7] M. Tobajas, E. Garcia-Calvo, Comparison of experimental methods for determination of the volumetric mass transfer coefficient in fermentation processes, Heat and Mass Transfer 36 (2000) 201–207.
[8] P. Van der Maas, T. van de Sandt, B. Klapwijk, P. Lens, Biological reduction of nitric oxide in aqueous Fe(II)EDTA solutions, Biotechnol. Prog. 19 (2003) 1323–1328.
[9] Standard Methods for the Examination of Water and Wastewater, 19th ed., American Public Health Association (APHA), Washington, DC, 1998.
[10] A.I. Vogel, Vogel's Textbook of Quantitative Chemical Analysis, Longman, London, 1978.
[11] A.A.C.M. Beenackers, W.P.M. van Swaaij, Mass transfer in gas–liquid slurry reactors, Chem. Eng. Sci. 48 (1993) 3109–3139.
[12] G. Quicker, E. Alper, W.D. Deckwer, Gas absorption rates in a stirred cell with plane interface in the presence of fine particles, Can. J. Chem. Eng. 67 (1989) 32–38.
[13] O. Okzan, A. Calimli, R. Berber, H. Oguz, Effect of inert solid particles at low concentration on gas–liquid mass transfer in mechanically agitated reactors, Chem. Eng. Sci. 55 (2000) 2737–2740.
[14] G.E.H. Joosten, J.G.M. Schilder, J.J. Janssen, The influence of suspended solid material on the gas liquid mass transfer in stirred gas–liquid contactors, Chem. Eng. Sci. 32 (1977) 563–566.
[15] M. Charles, Technical aspects of the rheological properties of microbial cultures Advances in Biochemical Engineering, vol. 8, Springer-Verlag, Berlin, 1978.
[16] K.R. Westerterp, W.P.M. van Swaaij, A.A.C.M. Beenackers, Chemical Reactor Design and Operation, Wiley, New York, 1984.
[17] M.V. Dagaonkar, Effect of a microphase on gas–liquid mass transfer. PhD thesis, RijksUniversiteit Groningen, The Netherlands, 2001.
[18] M. Vinke, P.J. Hamersma, J.M.H. Fortuin, The enhancement of gas absorption rate in agitated slurry reactors due to the adhesion of gas absorbing particles to bubbles, Chem. Eng. Sci. 47 (1992) 3589–3596.